

SUPPLEMENTAL DATA

Table S1. The CHD4 shRNA sequences used in this study

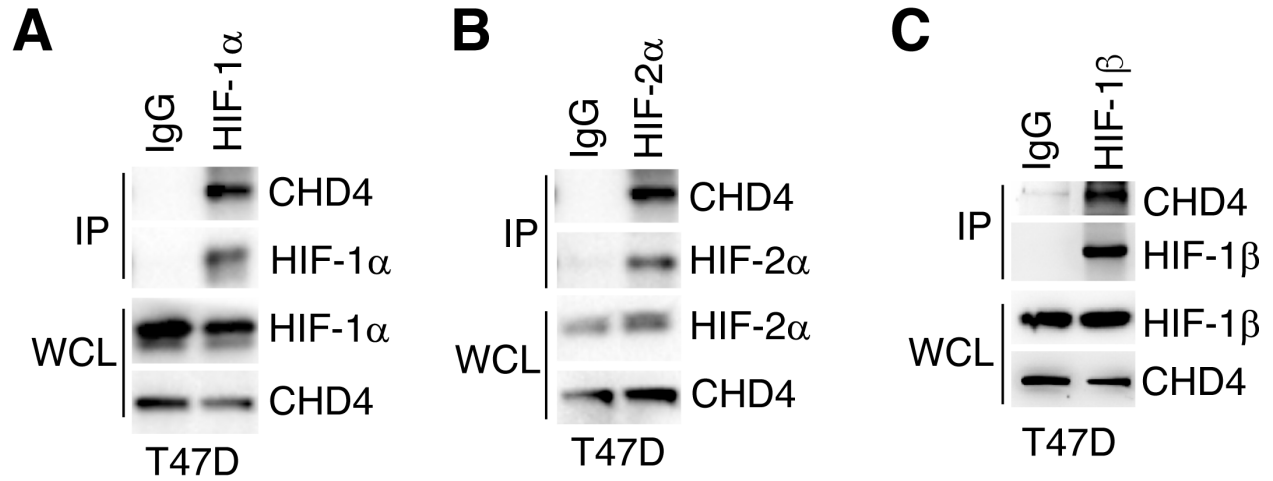
shCHD4#1	5'-GCGGGAGTTCAGTACCAATAA-3'
shCHD4#2	5'-CGAAGGTTTAAGCTCTTAGAA-3'

Table S2. The qPCR primers used in this study

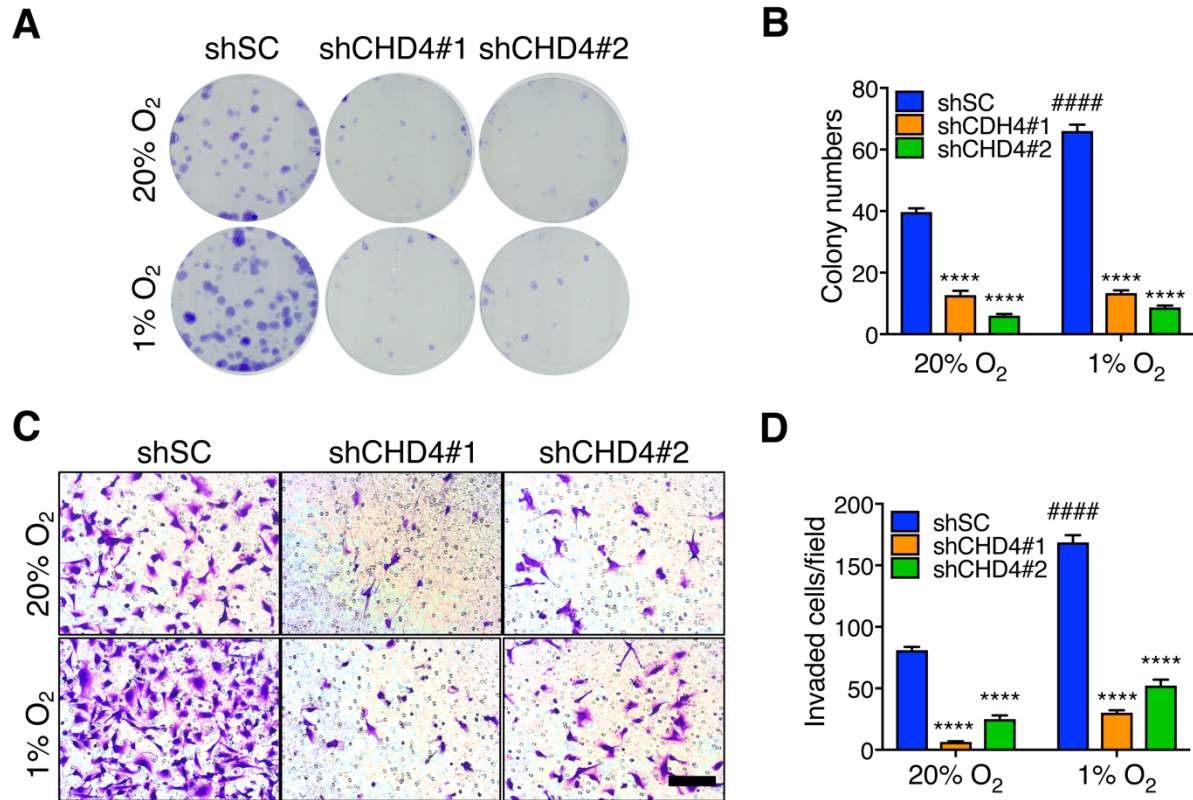
VEGFA mRNA	Forward: 5'-CTTGCCTTGCTGCTCTAC-3'
	Reverse: 5'-TGGCTTGAAGATGTACTCG-3'
LOX mRNA	Forward: 5'-CGGCGGAGGAAAACCTGTCT-3'
	Reverse: 5'-TCGGCTGGGTAAAGAAATCTGA-3'
18S rRNA	Forward: 5'-CGGCGACGACCCATTCGAAC-3'
	Reverse: 5'-GAATCGAACCCTGATTCCTCCGTC-3'
ANGPTL4 mRNA	Forward: 5'-GTCCACCGACCTCCCGTTA-3'
	Reverse: 5'-CCTCATGGTCTAGGTGCTTGT-3'
NDNF mRNA	Forward: 5'-ATCAGCCATACCCTGAGTTACC-3'
	Reverse: 5'-TGAATGGGTTGTTTCAGCAAAGA-3'
RPL13A mRNA	Forward: 5'-CTCAAGGTCGTGCGTCTG-3'
	Reverse: 5'-TGGCTTCTCTTTCCTCTTCTC-3'
ANGPTL4 HRE	Forward: 5'-ATTTGCTGTCCTGGCATC-3'
	Reverse: 5'-CCAGCTCATTCTCTGGAATC-3'
VEGFA HRE	Forward: 5'-CAGACTCCACAGTGCATAC-3'
	Reverse: 5'-AGTTTGTGGAGCTGAGAAC-3'
LOX HRE	Forward: 5'-GAAGATTTCTCCTTCCCTCAC-3'
	Reverse: 5'-GAAGCGCATCACTCCTTT-3'
RPL13A gDNA	Forward: 5'-GAGGCGAGGGTGATAGAG-3'
	Reverse: 5'-ACACACAAGGGTCCAATTC-3'

Table S3. Gene ontology analysis of CHD4-induced HIF target genes by the DAVID

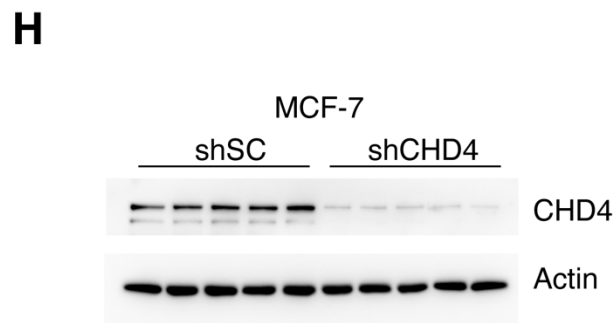
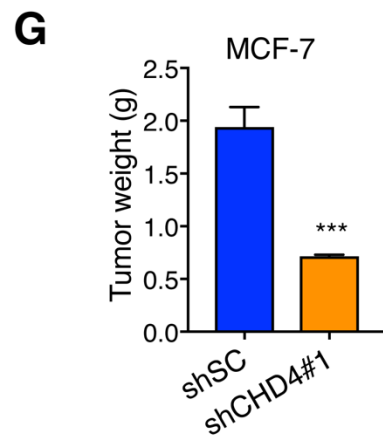
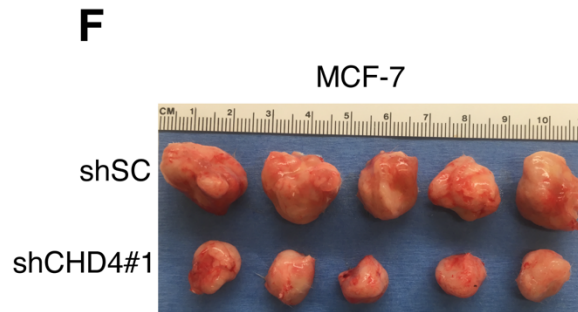
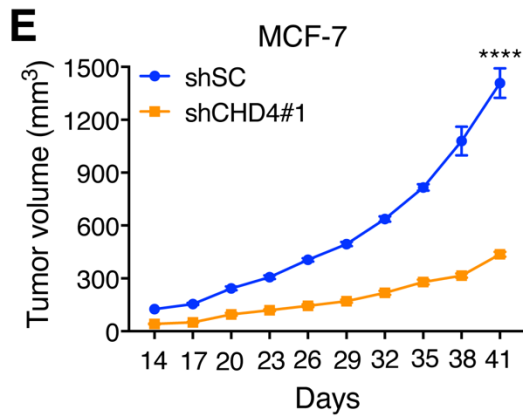
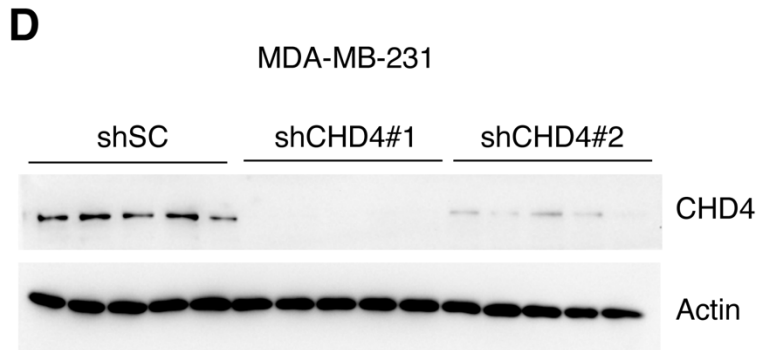
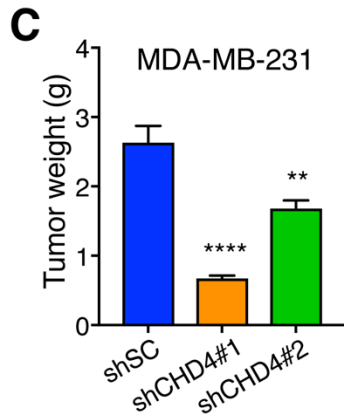
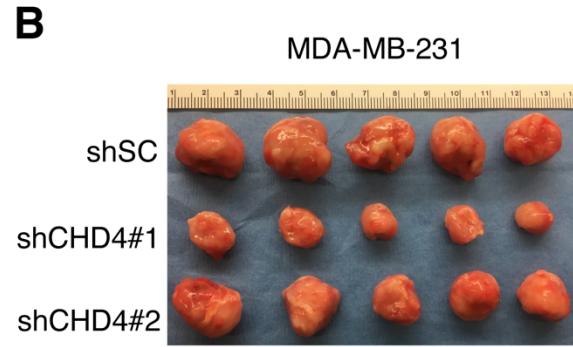
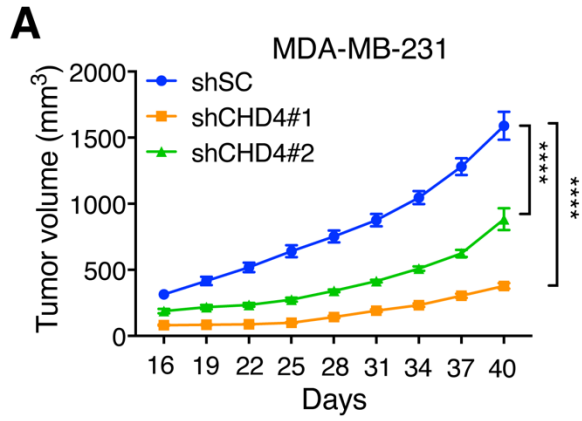
Biological Process	P-Value
angiogenesis	3.20E-07
response to hypoxia	2.00E-05
extracellular matrix organization	1.30E-03
collagen catabolic process	1.60E-03
cellular response to hypoxia	1.80E-03
positive regulation of apoptotic process	2.40E-03
positive regulation of nitric oxide biosynthetic process	2.50E-03
extracellular matrix disassembly	3.50E-03
positive regulation of neuron projection development	6.80E-03
negative regulation of cell proliferation	7.00E-03
semaphorin-plexin signaling pathway	9.50E-03
protein homooligomerization	9.70E-03
skeletal system development	1.00E-02
positive regulation of JNK cascade	1.10E-02
signal transduction	1.20E-02
cellular response to heat	1.30E-02
sphingolipid metabolic process	1.70E-02
positive regulation of angiogenesis	1.90E-02
cell-cell signaling	2.10E-02
response to drug	2.10E-02
positive regulation of actin filament polymerization	2.20E-02
wound healing	2.20E-02
positive regulation of MAPK cascade	2.30E-02
response to osmotic stress	2.40E-02
positive regulation of gene expression	2.50E-02
positive regulation of cell division	2.50E-02
positive regulation of protein kinase activity	2.50E-02
cell proliferation	2.50E-02
positive regulation of osteoclast differentiation	2.60E-02
negative regulation of phosphorylation	2.90E-02
positive regulation of NF-kappaB import into nucleus	3.10E-02
negative regulation of neuron apoptotic process	3.20E-02
positive regulation of NF-kappaB transcription factor activity	3.30E-02
positive regulation of cell migration	3.70E-02
positive regulation of neutrophil extravasation	3.90E-02
fever generation	3.90E-02
cell adhesion	4.50E-02
negative regulation of axon extension involved in axon guidance	4.70E-02
positive regulation of mitotic nuclear division	4.70E-02



Supplemental Figure S1. CHD4 interacts with HIF-1 and HIF-2 in breast cancer T47D cells. (A-C) Co-IP with IgG, anti-HIF-1 α (A), anti-HIF-2 α (B), or anti-HIF-1 β (C) antibody in T47D cells exposed to 1% O₂ for 6 hrs. WCL, whole cell lysate.



Supplemental Figure S2. CHD4 promotes colony formation and invasion of breast cancer cells. (A and B) Clonogenic assay in shSC and CHD4 KD MDA-MB-231 cells exposed to 20% or 1% O₂ for 14 days. Representative images from three independent experiments are shown in A. The data are quantified in B ($n = 3$, mean \pm SEM). **** $p < 0.0001$ vs. shSC, ##### $p < 0.0001$ vs. 20% O₂, by 2-way ANOVA with Turkey's test. (C and D) Invasion assay in shSC, CHD4 KD and rescued MDA-MB-231 cells exposed to 20% or 1% O₂ for 24 hrs. Representative images from four independent experiments are shown in C. The data are quantified in D ($n = 4$, mean \pm SEM). **** $p < 0.0001$ vs. shSC, ##### $p < 0.0001$ vs. 20% O₂, by 2-way ANOVA with Turkey's test. Scale bar, 100 μ m.



Supplemental Figure S3. CHD4 promotes breast tumor growth in mice. **(A-D)** shSC and CHD4 KD MDA-MB-231 cells were orthotopically implanted into the mammary fat pad of female NSG mice, respectively. Tumor growth curve **(A)**, image **(B)**, and weight **(C)** are shown ($n = 5$, mean \pm SEM). CHD4 KD in tumors was verified by immunoblot assay **(D)**. ** $p < 0.01$ by 1-way ANOVA with Dunnett's test. **** $p < 0.0001$, by 1-way ANOVA with Dunnett's test or 2-way ANOVA with Turkey's test. **(E-H)** shSC and CHD4 KD MCF-7 cells were orthotopically implanted into the mammary fat pad of female NSG mice, respectively. Tumor growth curve **(E)**, image **(F)**, and weight **(G)** are shown ($n = 5$, mean \pm SEM). CHD4 KD in tumors was verified by immunoblot assay **(H)**. *** $p < 0.001$ by Student's t test. **** $p < 0.0001$, by 2-way ANOVA with Sidak's test.